

Article

Machine learning model for predicting symptom improvement rates in hospitalized deep vein thrombosis patients

Nan Zhou¹, Teck Han Ng¹, Chai Nien Foo¹, Lloyd Ling², Yang Mooi Lim^{1*}

¹M. Kandiah Faculty of Medicine and Health Science, Universiti Tunku Abdul Rahman, Kajang, Selangor 43000, Malaysia

²Lee Kong Chian Faculty of Engineering and Science, Universiti Tunku Abdul Rahman, Kajang, Selangor 43000, Malaysia

ARTICLE INFO

Article history:

Received 30 August 2025

Received in revised form

06 October 2025

Accepted 01 December 2025

Keywords:

Deep vein thrombosis, Machine learning,

Treatment response prediction,

Clinical decision support

*Corresponding author

Email address:

ymlim@utar.edu.my

DOI: [10.55670/fpl.futech.5.1.22](https://doi.org/10.55670/fpl.futech.5.1.22)

ABSTRACT

Deep Vein Thrombosis (DVT) demonstrates considerable treatment response heterogeneity, with 40-60% of patients developing complications despite standard anticoagulation therapy. Accurate prediction of individual treatment outcomes remains an unmet clinical need. This study develops and validates a machine learning-based model to predict symptom Improvement Rate (IPR) using retrospective data from 403 hospitalized DVT patients (2018-2023). Six predictive features are identified using Random Forest-based Recursive Feature Elimination (RFE): age, white blood cell count, Activated Partial Thromboplastin Time (APTT), Thrombin Time (TT), surgical intervention status, and baseline symptom severity. The regularized eXtreme Gradient Boosting (XGBoost) algorithm achieves optimal performance with a test coefficient of determination (R^2) of 0.60, Root Mean Square Error (RMSE) of 12.36, and five-fold cross-validation R^2 of 0.58 ± 0.07 . SHapley Additive exPlanations (SHAP) analysis reveals that APTT and surgical intervention are the strongest predictors of treatment response. The validated model is deployed as a publicly accessible web-based clinical decision support tool, enabling real-time outcome prediction at the point of care. This research establishes a practical framework bridging predictive analytics and clinical practice, facilitating evidence-based, personalized DVT management strategies.

1. Introduction

DVT = Deep Venous Thrombosis (DVT) refers to deep vein thrombosis, a type of venous system disease. Most often, it occurs in deep veins. It is mainly in the deep veins of the limbs, especially the lower extremities, and can extend to the pelvic veins and the lower half of the inferior vena cava [1]. DVT's incidence among hospitalized patients rises considerably, reaching 100 - 200 for every 100,000 persons yearly all over the world, with much higher numbers in certain populations, post-surgical patients (2-3%), critically ill patients (5-10%), and those with malignancies (4-20%) [2-4]. The classical presentation includes unilateral limb edema/pain, erythema, and warmth; however, ~30% are clinically silent until complications [5,6]. Mature anticoagulation therapy protocols have been established, including low-molecular-weight heparin, direct oral anticoagulants, and vitamin K antagonists. However, there are still considerable differences in individual responses to the therapy, which are related to different genetic variations, comorbidities, and interactions with the medicine [7,8]. Clinical evidence shows that after standard treatment,

between 40% and 60% of DVT patients still have a risk of complications like post-thrombotic syndrome. The symptoms of this syndrome include chronic leg pain, swelling, skin changes, and, in the worst cases, venous ulcers, all of which can seriously reduce a person's quality of life and use more medical resources [9]. This heterogeneity necessitates early identification of treatment-resistant patients to enable timely intervention with advanced therapies, including catheter-directed thrombolysis, mechanical thrombectomy, or extended anticoagulation regimens [10]. In recent years, machine learning technology has made great progress in the field of health care, especially in predicting disease prognosis and evaluating symptom improvement [11]. The traditional treatment response assessment for DVT mainly relies on clinical experience and single-parameter judgment, without sufficient consideration of individual patients and multidimensional clinical data [12,13]. Machine learning algorithms include the demographic aspect of laboratory results, images, and therapy, and produce better forecast models. Studies demonstrate that machine learning approaches outperform conventional statistical methods in

predicting thrombotic events [14, 15]. The goal is to develop a machine learning-based prediction model to assess the response of DVT treatment with regard to symptom improvement rate among hospitalized DVT patients. We incorporate patients' clinical characteristics, laboratory parameters, and treatment parameters to construct a multi-dimensional model. The model aims to accurately predict an individual patient's treatment improvement rate to assist clinicians in personalizing treatment plans. Furthermore, this study identifies key factors influencing symptom improvement, providing evidence-based guidance for therapeutic optimization.

2. Methods

2.1 Research design

This study was conducted in accordance with the TRIPOD statement. The completed TRIPOD checklist is provided as Supplementary File 2. This retrospective observational study utilizes real-world data from the comprehensive hospital information system of [Masked for blind review] to evaluate treatment outcomes in patients diagnosed with DVT from 2018 to 2023. Specific inclusion and exclusion criteria were applied to ensure data completeness and relevance. Inclusion criteria: (1) DVT is the main diagnosis in medical records; (2) complete medical records required for the study are available. Complete medical records were defined as containing: (1) ultrasound-confirmed DVT diagnosis; (2) baseline and discharge symptom scores; (3) laboratory data within 24 hours of admission; (4) therapeutic intervention records; and (5) documented outcomes. Planned diagnostic and treatment procedures referred to completion of the institutional protocol without premature discontinuation. Exclusion criteria: (1) Incomplete planned diagnostic and treatment procedures during hospitalization due to reasons such as transfer or treatment abandonment; (2) Unavailable data on confounding factors in medical records due to attending physician resignation or retirement.

Between January 2018 and December 2023, 658 patients were identified. After excluding 215 patients (150 incomplete records, 65 transfers), 443 remained eligible. Subsequently, 40 patients with missing confounding variables were excluded, leaving 403 patients in the final cohort (Figure 1). Cases meeting these criteria were systematically entered into an electronic data collection form designed specifically for this study. The data collection protocol encompasses a comprehensive set of variables (Supplementary File Table 1), including: patient hospitalization identification number (utilized solely for Source Data Verification purposes), demographic characteristics, hematological and coagulation function parameters assessed on the initial day of admission, duration of symptoms before admission, ultrasound-confirmed thrombus localization, admission Wells score, history of DVT and associated comorbidities, therapeutic interventions for DVT and concomitant conditions (encompassing both pharmacological and physical modalities), surgical management strategies and a reference Diagnostic and Efficacy Criteria for Deep Venous Thrombosis of the Lower Extremities (Revised in 2015) symptom quantification assessment (Supplementary File Table 1) [16]. All patient identifiers were removed prior to analysis. Data extraction and de-identification were performed by personnel independent of the analytical team. This study was approved by the Ethics Committee of The Sun Simiao Hospital of Beijing University of Chinese Medicine (Approval number:

SSMYY-KYPJ-2023-011). It conforms to the ethical standards of medical research.

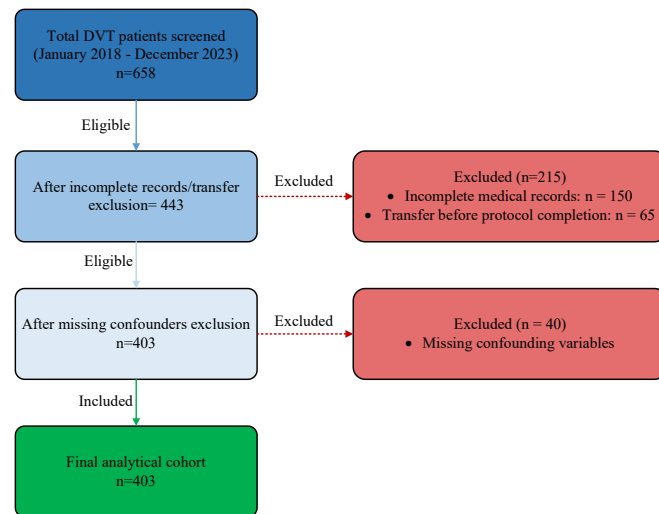


Figure 1. Sequential patient selection flow diagram

2.2 Data preprocessing and exploratory analysis

Key variables included demographic data (age, sex), laboratory parameters (WBC, APTT, TT), therapeutic interventions, and symptom severity scores. Data cleaning processes attended to natural missingness via systematic imputation and deletion methods. Variables that had less than 30% missing values were subjected to KNN imputation. KNN was implemented with $k=5$ neighbors using Euclidean distance for numerical variables and Hamming distance for categorical variables. Those above this figure were eliminated to avoid any form of analytical bias. The 30% threshold follows established guidelines for clinical prediction models. No variables exceeded this threshold. The final six features all demonstrated minimal missingness below the threshold. Disease classifications were standardized using ICD-10-CM coding, and drug names were unified systematically (specific formulations were converted to general names). The hospital system used ICD-10-CM natively; no manual mapping was required. Binary variables were coded as 0/1, ordinal variables were retained with their natural ordering, and one-hot encoding was avoided due to sample size constraints. Continuous variables were standardized to avoid unit-based changes. Descriptive statistics of the dataset characteristics, with a summary of continuous variables including minimum value, maximum value, and median value; and a summary of categorical variables using frequency distributions. Skewness, kurtosis, and the disparity ratio are computed to evaluate the distribution of the data and identify potential limitations of the models, laying the groundwork for subsequent analytical activities.

2.3 Variable definition

This study used the Improvement Rate (IPR) to assess symptom improvement. $IPR = [(Day\ 1\ symptom\ score - discharge\ symptom\ score) / Day\ 1\ symptom\ score] \times 100\%$, which indicates the percentage of symptom severity reduction from onset to discharge. Symptom scores (0-12 points) were assessed using the 2015 DVT Diagnostic Criteria, evaluating swelling, pain, skin changes, and function. Patients with zero baseline scores were excluded; IPR was capped at 100%. This standard measurement allows objective assessment of symptom resolution in the patient group.

2.4 Model development and evaluation

The dataset was split 80 - 20 on the train-test sets. Five-fold cross-validation was performed on the training set to ensure robust performance estimation. A MinMax scaler was applied to normalise the data to the range [0,1]. Feature selection used the RFE from the random forest model, checking model performance with 3-12 kept features to determine the best feature set size. RFE employed Random Forest with 100 estimators, using R^2 as the selection metric. No significant multicollinearity was detected among retained features (VIF < 5).

Four models were implemented: linear regression, SVR, random forest and xgboost. Hyperparameter optimization was conducted using the Optuna framework to optimize the model. For XGBoost, the search space included: learning_rate (0.01-0.3), max_depth (3-8), n_estimators (50-300), subsample (0.6-1.0), colsample_bytree (0.6-1.0), reg_alpha (0-10), and reg_lambda (1-10). Optimized parameters were: learning_rate=0.01, max_depth=3, n_estimators=150, subsample=0.8, colsample_bytree=0.8, reg_alpha=5.0, reg_lambda=10.0. Early stopping with 30 rounds was applied to prevent overfitting.

Model evaluation metrics included the coefficient of determination (R^2), Mean Squared Error (MSE), Mean Absolute Error (MAE), and Root Mean Squared Error (RMSE) to evaluate the model's performance across diverse modeling strategies. Bootstrap resampling (1000 iterations) was used to estimate 95% confidence intervals for all performance metrics. Model calibration was assessed using calibration plots (Figure 2). The calibration slope was 0.84, calibration-in-the-large was 8.43, and the Brier score was 0.006, indicating acceptable calibration with minor systematic bias.

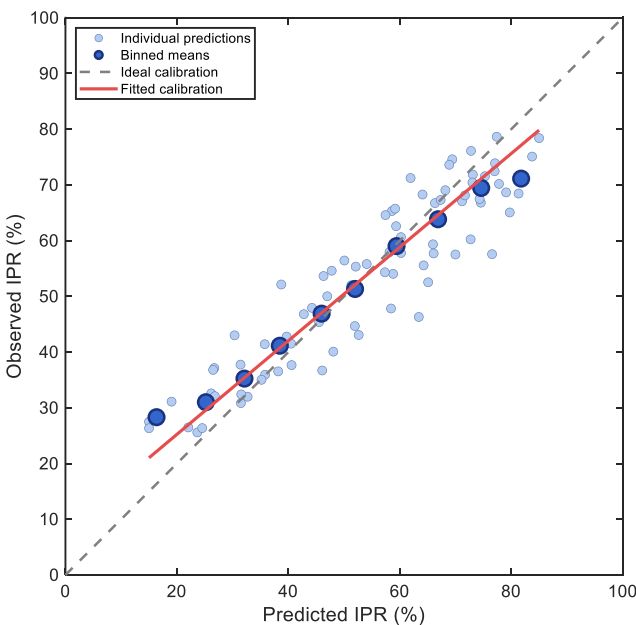


Figure 2. Calibration plot for XGBoost model

2.5 Model interpretation

SHAP (SHapley Additive exPlanations) analysis was performed on the optimal performing model to explore features. TreeExplainer was used for SHAP value computation, which is optimized for tree-based ensemble methods including XGBoost. Values are calculated using cooperative game theory and measure a feature's marginal

contribution to model predictions by averaging the effects of all possible feature combinations. It delivers both global feature importance ratings and local understandability for separate predictions. The SHAP framework assigns each feature a value that reflects its importance for the model's outputs. It shows how features interact and influence model output without losing accuracy. It helps people see how models make decisions. In this analysis of explainable results, we gain essential knowledge of the patterns behind the model's decisions, enabling us to transform those mathematical results into useful information for clinics.

2.6 Model deployment

To make it easier for doctors to use, we made a simple computer program using a tool called Gradio. This program is like a window where doctors can see the results of our model in a way that's easy for them to understand. The interface was deployed to the Hugging Face platform and is publicly available to any healthcare practitioners. The model is accessible at https://huggingface.co/spaces/Curvature/DVT_Management. Source code, trained model, and environment specifications (Python 3.9, XGBoost 1.7.0, random seed 42) are available on GitHub. Users must confirm healthcare professional status before accessing. This deployment strategy overcomes technical obstacles, allowing for immediate use of the model without specialized programming skills. The whole project, together with its source code and documentation, was published under the MIT license, promoting open collaboration and enabling everyone to freely modify and distribute it. It ensures that the know-how is widely known, so it can be easily used when caring for sick people, connecting what researchers discover with how doctors actually care for patients.

3. Results

3.1 Descriptive statistics

The study population comprised 403 patients with a mean age of 61.32 ± 14.84 years, and anthropometric measurements were done for the same, with an average height of 161.37 ± 6.89 cm and weight of 61.43 ± 10.77 kg. Males accounted for 54.09% and females for 45.91%. Comprehensive laboratory parameters revealed mean values of WBC $9.90 \pm 2.15 \times 10^9/L$, RBC $5.04 \pm 0.37 \times 10^{12}/L$, Hgb $15.03 \pm 1.07 g/dL$, PLT $165.20 \pm 64.74 \times 10^9/L$, and HCT $45.10 \pm 1.42\%$, suggesting mild leukocytosis with otherwise normal hematological profiles. Coagulation profiles showed PT $13.29 \pm 1.93 s$, INR 1.09 ± 0.17 , APTT $32.94 \pm 5.08 s$, TT $25.69 \pm 5.17 s$, Fibrinogen $3.53 \pm 0.87 g/L$, D-dimer $12.30 \pm 4.91 mg/L$, and FDP $19.49 \pm 10.45 mg/L$, indicating hypercoagulability with markedly elevated D-dimer and FDP levels characteristic of venous thromboembolism.

Thrombus locations predominantly involved the popliteal vein (55.58%), common femoral vein (52.36%), iliac vein (45.16%), posterior tibial vein (43.92%), and inter-muscular veins of the calf (37.97%). Percentages exceed 100% as patients frequently presented with multi-site involvement, demonstrating extensive thrombosis of both proximal and distal lower extremity vasculature. Therapeutic Management was comprehensive. Enoxaparin 62.78% was the most common medication, followed by Diosmin 44.67%, and Rivaroxaban 37.22%. Treatment protocols followed institutional guidelines; therapeutic variations were accounted for in model development through inclusion of intervention status as a predictor variable. Non-pharmacological therapies were limb elevation at 30 degrees

(73.70%), Bingxiao external application (46.65%), and compression stockings (35.73%). Most procedures performed are Venography (70.97%), Therapeutic Treatment (Thrombolysis, Thrombectomy) (70.47%), Filter Placement/Retrieval (47.89%), Angioplasty / Stent (33.00). The comorbidity analysis showed that essential hypertension (28.54%), type 2 diabetes mellitus (14.64%), and other venous disorders (11.91%) were the most common, with 13.65% of patients having no comorbidities. The occupational distribution showed farmers (26.55%), unemployed individuals (23.08%), and retired persons (11.41%) as the major parts of the cohort, possibly indicating socio-economic elements related to DVT creation and management.

3.2 Feature selection

RFE analysis was performed to improve feature selection, and R^2 was evaluated across different feature subsets. The R^2 curve showed optimal performance between 6 and 8 features, with a maximum R^2 of 0.58. 6 Key predictors were selected. The final feature set comprised one demographic parameter (age), three laboratory parameters (white blood cell count, activated partial thromboplastin time, thrombin time), one therapeutic parameter (thrombolysis/thrombectomy), and one clinical parameter (Day 1 symptom score). Feature definitions were as follows: age (years), WBC ($\times 10^9/L$), APTT (seconds), TT (seconds), thrombolysis/thrombectomy (binary, 1=performed), and Day 1 symptom score (0-12 points). These features were the most influential predictors that kept the model efficient (Figure 3).

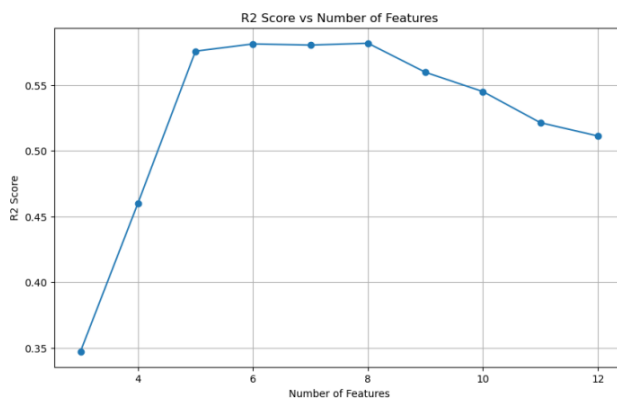


Figure 3. Feature selection optimization: R^2 performance analysis across varying feature dimensions

3.3 Model evaluation

A comparison of the four machine learning models shows different performances on both training and testing datasets. The overall assessment of prediction accuracy via true-versus-predicted scatter plots shows that XGBoost reached the best alignment with the ideal diagonal line, meaning that it has the strongest predictive ability and the least systematic bias. After applying regularization to address overfitting, XGBoost achieved a test R^2 of 0.60, RMSE of 12.36, and five-fold cross-validation R^2 of 0.58 ± 0.07 . The second-best model was Random Forest, and it had an R^2 of 0.573 and an RMSE of 12.77. The residuals were fairly spread out across all of the predictions, but they were slightly more scattered than the XGBoost model. On the other hand, both the Linear Regression and Support Vector Machine models yielded much worse results, with test R^2 values of 0.333 and 0.242, respectively, indicating a poor ability to model the underlying

pattern in the data. Their corresponding residual plots showed obvious heteroscedasticity (Breusch-Pagan test, $p < 0.05$), especially in areas with high predictions, where large deviations from the actual values were observed, suggesting a systematic error in prediction that increases with the size of the target. Detailed residual analysis again showed that XGBoost has better prediction stability, with the most concentrated and symmetrical residual distribution centered on 0, few outliers, and consistent error variation across the entire prediction range. This stability is quantified by XGBoost's test-set MAE of 7.82 and MSE of 152.80, the smallest errors among all models. After regularization, the gap between training R^2 (0.75) and test R^2 (0.60) was reduced to 0.15, compared to 0.35 before regularization, demonstrating effective mitigation of overfitting. This improved generalization makes the model suitable for clinical deployment. Random Forest showed a larger train-test gap (training R^2 of 0.9396 versus test R^2 of 0.5729). Both the quantitative performance metrics and the graphical diagnostics from the scatter and residual plots support selecting XGBoost as the best model to deploy in a clinical setting for providing the most accurate predictions of symptom improvement rate in DVT patients (Figure 4-7; Table 1). Temporal validation was performed by training on 2018-2021 data and testing on 2022-2023 data, yielding comparable performance ($R^2=0.61$), supporting model generalizability. Decision curve analysis demonstrated positive net benefit across threshold probabilities of 30-70%, indicating clinical utility compared to default strategies.

Table 1. Performance metrics comparison of machine learning models for prediction across training and test sets

Model	Dataset	R^2	5-Fold CV R^2	MSE	RMSE	MAE
XGBoost(Regularized)	Train	0.7500	0.58 ± 0.07	104.05	10.20	6.85
	Test	0.6000	-	152.80	12.36	7.82
Random Forest	Train	0.9396	0.52 ± 0.08	25.12	5.01	2.85
	Test	0.5729	-	163.18	12.77	8.11
Linear Regression	Train	0.4874	0.31 ± 0.05	213.31	14.61	9.62
	Test	0.3333	-	254.72	15.96	10.59
SVM	Train	0.3802	0.22 ± 0.06	257.88	16.06	10.95
	Test	0.2417	-	289.75	17.02	11.01

3.4 SHAP analysis

SHAP analysis showed different patterns of feature importance and its impact on the model-predicted IPR. APTT had the biggest impact on the model, with SHAP values going between -15 and +15, high APTT values were associated with lower IPR predictions, which may reflect clinical considerations regarding bleeding risk. Surgical intervention (T&T) had a clear bimodal distribution. Positive T&T was associated with greater IPR prediction (SHAP values +10 to +15) as it indicated the benefit of early thrombus removal, and negative T&T was associated with lesser IPR prediction (SHAP values -10 to -15). WBC count had a moderate bilateral impact: low counts (SHAP values -5 to 0) predicted good outcomes by lowering inflammation, and high counts (SHAP values 0 to +5) predicted poor outcomes.

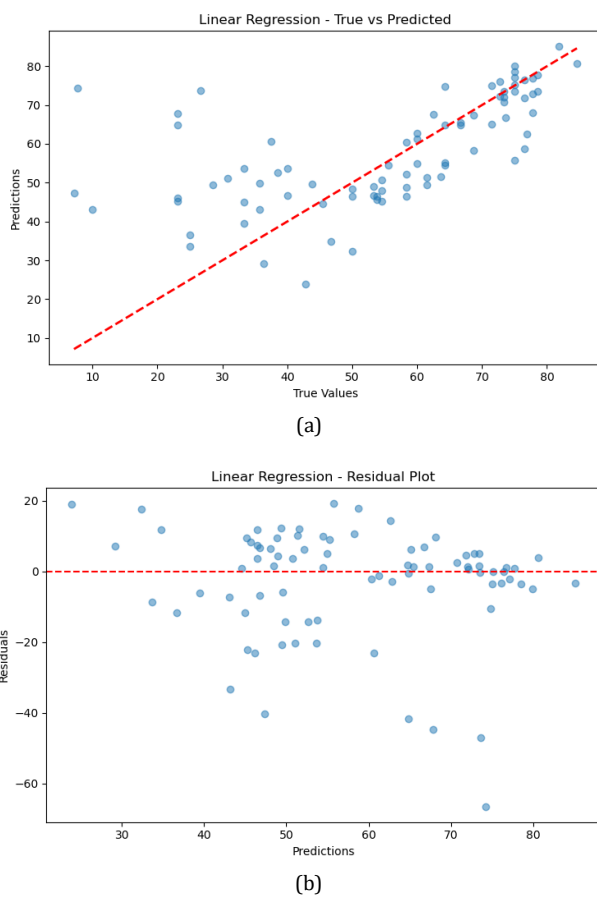


Figure 4. Linear regression: predictive accuracy assessment through (a) true-predicted correlation, (b) residual distribution analysis

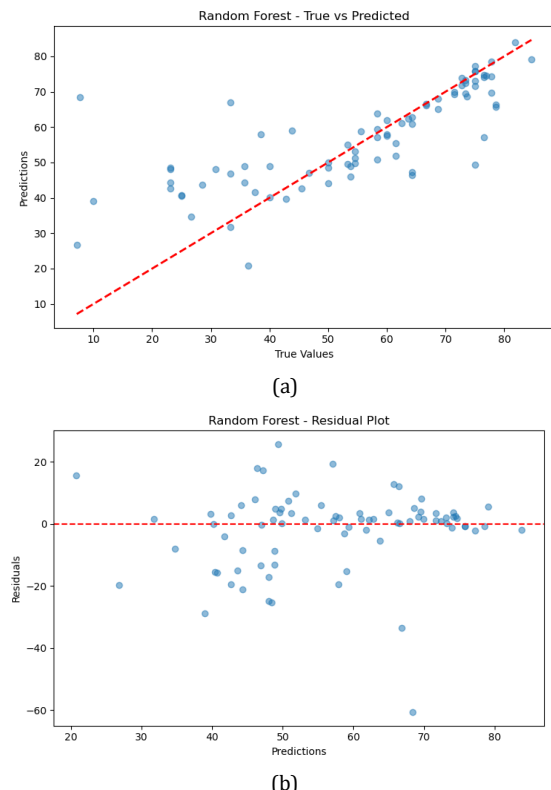


Figure 5. Random forest: predictive accuracy assessment through (a) true-predicted correlation, (b) residual distribution analysis

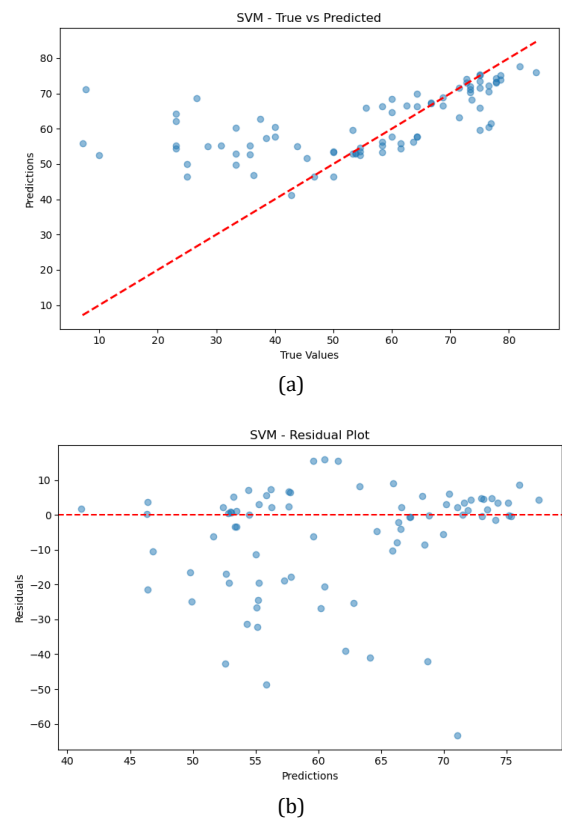


Figure 6. Support vector machine: predictive accuracy assessment through (a) true-predicted correlation (b) residual distribution analysis

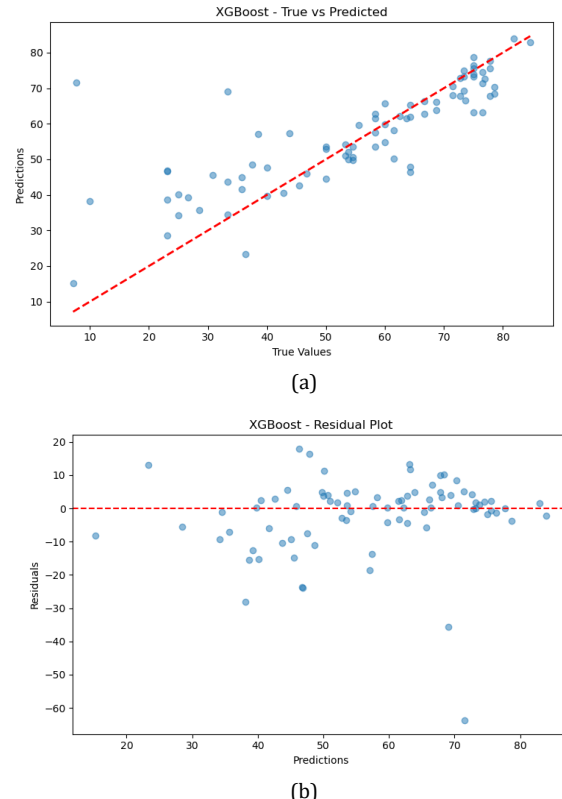


Figure 7. XGBoost: Predictive accuracy assessment through (a) true-predicted correlation (b) residual distribution analysis

Age showed asymmetric SHAP values between -5 and +10, with older age having a negative effect on IPR prediction, as older patients have less tolerance for treatments and more complications. The initial symptom scores displayed balanced bidirectional impacts, with zero as the center, and severe baseline symptoms indicating a larger possible margin of improvement. TT has the most concentrated distribution, indicating stabilization of the predictions. Parallel coordinate visualization validated these associations; optimal IPR predictions (80 - 100 %) showed low APTT, positive surgical status, and moderate WBCs, poor outcomes (20 - 40 %) linked to high APTT, negative surgical status, and poor inflammation markers (Figure 8 and Figure 9).

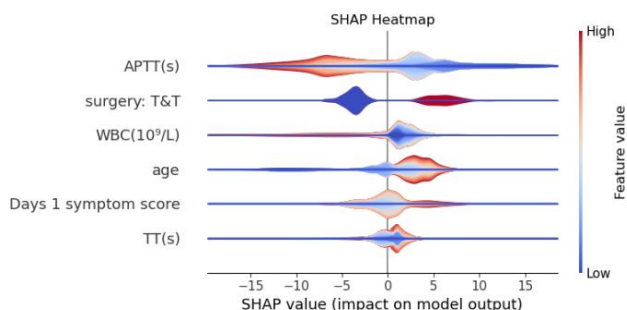


Figure 8. Feature impact distribution analysis through SHAP value visualization

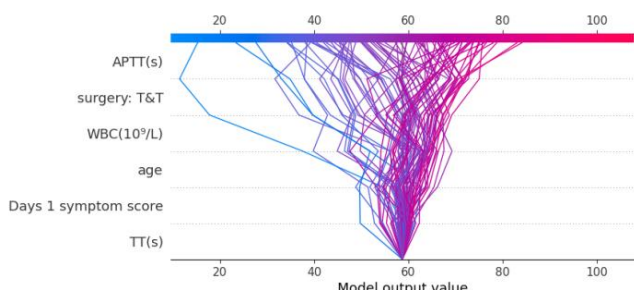


Figure 9. Model output response analysis with feature value distribution

3.5 User interface development and deployment

Deployed DVT Symptom Improvement Management System with Predictive Analytics into Clinical Workflow via a Web-based Platform. This implementation takes multidimensional clinical parameters, labs, and standardized symptom evaluation and creates a quantitative measure of the rate of improvement. The system uses SHAP-based model interpretation, and the clinicians can see which parameters contribute the most to the model's predictions. This evidence-based decision-support framework aids risk stratification, therapeutic strategy enhancement, and outcome prediction in the management of DVT. Implementing the platform in clinical assessment would lead to more consistent assessment of the patient's current state, generating data-driven information to build a tailored treatment plan. This implementation bridges the translation gap between high-end machine learning algorithms and clinical practice and establishes a standard method for predicting evidence-based DVT symptom improvement in routine medical care (Supplementary File Figure 2).

4. Discussion

This study developed and validated a machine learning-based prediction model of DVT symptom improvement rates, achieving good predictive performance in the test set ($R^2 = 0.60$). Among the four machine learning methods, the XGBoost algorithm had the best performance with an RMSE of 12.36 and an MAE of 7.82. By SHAP analysis, 6 key predictive features were identified, with APTT and whether surgery is performed being the most influential ones. It is successfully applied as a web-based clinical decision support system that can predict the improvement rate of symptoms in real time. These findings provide a novel approach to predicting individual treatment response in DVT patients by integrating multiple clinical parameters into an accessible decision support framework.

Deep vein thrombosis management is complicated by disease complexity, variable treatment responses, and potential serious complications. Treatment modalities include anticoagulant therapy, thrombolysis, and mechanical interventions, each producing different effects depending on patient characteristics and treatment compliance. Low-molecular-weight heparin (LMWH) is effective for both proximal and isolated distal DVT [17]. However, anticoagulation response varies considerably among patients, influenced by age, weight, renal function, and pharmacogenetic factors [18]. Elderly patients exhibit altered pharmacokinetics, requiring careful monitoring and dose adjustment to maintain therapeutic levels while minimizing bleeding risk [19].

Surgical strategy significantly influences treatment outcomes. Catheter-directed thrombolysis (CDT) is recommended as first-line treatment for acute lower extremity DVT in patients with high thrombus burden [20]. However, procedural complications, including bleeding and embolization, may occur, potentially leading to post-thrombotic syndrome (PTS) [21]. Clinical studies demonstrate that multimodal intervention protocols achieve significantly lower PTS rates compared to anticoagulation alone [22, 23]. Treatment adherence is a critical prognostic determinant; sustained anticoagulation compliance maintains therapeutic efficacy and reduces recurrent thromboembolic risk [24]. However, treatment complexity, adverse effects, and limited patient awareness often compromise adherence [25]. These challenges underscore the clinical significance of standardized decision support tools to enhance physician-patient communication and improve treatment compliance.

This study established a machine learning-based symptom recovery prediction model within a web application framework, creating a clinical decision support system. Using the SHAP analysis methodology, the model displayed the contributions of the clinical indicators and the mechanisms that affected the results. From the SHAP value analysis, there is a significant negative correlation between APTT and IPR, suggesting that elevated APTT may be associated with reduced treatment efficacy. This relationship may reflect considerations in clinical decision-making, as elevated APTT indicates increased bleeding risk, potentially leading clinicians to adopt more conservative therapeutic approaches [7, 26]. Surgical intervention (thrombolysis/thrombectomy) emerged as a strong positive predictor, likely attributable to the benefits of early thrombus removal. Existing studies have shown that patients who underwent surgical interventions had better symptom improvement than those who did not, especially at earlier stages of the disease. This finding

supports the clinical value of early, personalized surgical decision-making [27].

WBC is an important inflammatory marker that indicates the level of inflammation, which is an important factor in the development of DVT clinical limb symptoms. This study found that lower initial WBCs were associated with better treatment response, which may be explained by thrombus-inflammation interactions. After a thrombus is formed, injured vascular endothelial cells and platelets will produce pro-inflammatory cytokines to attract leucocytes that invade the vessel wall. Activated leukocytes go on to release more cytokines and proteases, which can make the endothelial damage worse and lead to more reactions that cause blood to clot. Moreover, the released NETs directly take part in thrombosis and stimulate platelets to be activated, thus forming a vicious circle of inflammation-thrombosis and causing aggravated local tissue injury and continued clinical manifestations. Thus, lower WBC levels may indicate milder inflammatory responses and lesser thrombosis-inflammation cycle, which explains its link to better treatment response [28, 29].

Implementing a graphical user interface represents a significant advancement in translating machine learning algorithms into practical clinical tools [30]. The web-based platform reduces implementation barriers by eliminating requirements for specialized programming skills or computational infrastructure [31]. Interactive SHAP visualization transforms mathematical predictions into clinically interpretable information, enabling clinicians to understand both predictions and underlying reasoning [32]. This addresses the "black box" perception that undermines clinician confidence by providing a clear visualization of each parameter's influence through intuitive force plots [33]. The dynamic interface allows variable adjustment with immediate prediction updates, creating a simulation-like experience for treatment planning [34]. The system distinguishes modifiable from non-modifiable factors, guiding clinical attention toward areas with the greatest potential impact [35]. This transforms the model from a passive assessment tool into an active decision aid supporting personalized treatment optimization. This study has some limitations. As a single-center retrospective study at The Sun Simiao Hospital of Beijing University of Chinese Medicine, it is uncertain if our findings are generalizable to other regions or healthcare settings. Retrospective data collection may have selection bias. It may impact the robustness of our results even with thorough inclusion/exclusion criteria. In addition, we examined only in-hospital outcomes at discharge. We did not use long-term follow-up data to assess the model's forecasting performance for longer-term treatments and complications.

5. Conclusion

This study develops a new machine learning approach to predict DVT treatment response and demonstrates that this method has a better predictive performance than other methods through the XGBoost algorithm with an R² of 0.60 and an RMSE of 12.36. Comprehensive SHAP analysis revealed that APTT level and surgical intervention are major factors determining the outcome of treatment, providing essential information on the mechanism of DVT treatment response. We have successfully deployed our model as a web-based clinical decision support tool. This is a major advance in taking complex algorithmic predictions and putting them to practical use in a clinical setting. This implementation connects theory with real-world medicine, providing doctors

with a common, proven method to figure out how well their patients will respond to treatment. Our findings help understand how DVT is treated and set a basis for personal ways to treat DVT.

Ethical issue

The authors are aware of and comply with best practices in publication ethics, specifically regarding authorship (avoidance of guest authorship), dual submission, manipulation of figures, competing interests, and compliance with research ethics policies. The authors adhere to publication requirements that the submitted work is original and has not been published elsewhere.

Data availability statement

The manuscript contains all the data. However, more data will be available upon request from the authors.

Conflict of interest

The authors declare no potential conflict of interest.

References

- [1] S. Wolf et al., "Epidemiology of deep vein thrombosis," *Vasa*, 2024. doi: 10.1024/0301-1526/a001145
- [2] G. Wagner et al., "Prevalence and incidence of venous thromboembolism in geriatric patients admitted to long-term care hospitals," *Scientific reports*, vol. 14, no. 1, p. 17737, 2024. doi:10.1038/s41598-024-67480-1
- [3] S. Cheng et al., "Analysis of risk factors of postoperative lower extremity deep venous thrombosis in patients with cervical cancer," *Clinical and Applied Thrombosis/Hemostasis*, vol. 30, p. 10760296241240747, 2024. doi:10.1177/10760296241240747
- [4] J. Björklund et al., "Risk of venous thromboembolic events after surgery for cancer," *JAMA network open*, vol. 7, no. 2, pp. e2354352-e2354352, 2024. doi:10.1001/jamanetworkopen.2023.54352
- [5] M.-E. Mathieu et al., "Management and outcomes of superficial vein thrombosis: a single-center retrospective study," *Research and Practice in Thrombosis and Haemostasis*, vol. 8, no. 1, p. 102263, 2024. doi:10.1016/j.rpth.2023.102263
- [6] M. Betensky et al., "Recommendations for standardized definitions, clinical assessment, and future research in pediatric clinically unsuspected venous thromboembolism: communication from the ISTH SSC subcommittee on pediatric and neonatal thrombosis and hemostasis," *Journal of Thrombosis and Haemostasis*, vol. 20, no. 7, pp. 1729-1734, 2022. doi:10.1111/jth.15731
- [7] B. Cross, R. M. Turner, J. E. Zhang, and M. Pirmohamed, "Being precise with anticoagulation to reduce adverse drug reactions: are we there yet?," *The pharmacogenomics journal*, vol. 24, no. 2, p. 7, 2024. doi:10.1038/s41397-024-00329-y
- [8] A. Kholmukhamedov, D. Subbotin, A. Gorin, and R. Ilyassov, "Anticoagulation management: current landscape and future trends," *Journal of Clinical Medicine*, vol. 14, no. 5, p. 1647, 2025. doi:10.3390/jcm14051647
- [9] L. Khider et al., "Acute phase determinant of post-thrombotic syndrome: A review of the literature,"

Thrombosis Research, vol. 238, pp. 11-18, 2024.
doi:10.1016/j.thromres.2024.04.004

[10] M. R. Gil, J. Pantanowitz, and H. H. Rashidi, "Venous thromboembolism in the era of machine learning and artificial intelligence in medicine," *Thrombosis Research*, vol. 242, p. 109121, 2024.
doi:10.1016/j.thromres.2024.109121

[11] S. A. Alowais et al., "Revolutionizing healthcare: the role of artificial intelligence in clinical practice," *BMC medical education*, vol. 23, no. 1, p. 689, 2023.
doi:10.1186/s12909-023-04698-z

[12] A.-D. Anghel, V. Marina, L. Dragomir, C. A. Moscu, M. Anghel, and C. Anghel, "Predicting Deep Venous Thrombosis Using Artificial Intelligence: A Clinical Data Approach," *Bioengineering*, vol. 11, no. 11, p. 1067, 2024. doi:10.3390/bioengineering1111067

[13] K. Nothnagel and M. F. Aslam, "Evaluating the benefits of machine learning for diagnosing deep vein thrombosis compared with gold standard ultrasound: a feasibility study," *BJGP open*, vol. 8, no. 4, 2024.
doi:10.3399/BJGPO.2024.0057

[14] W. Sheng, X. Wang, W. Xu, Z. Hao, H. Ma, and S. Zhang, "Development and validation of machine learning models for venous thromboembolism risk assessment at admission: a retrospective study," *Frontiers in Cardiovascular Medicine*, vol. 10, p. 1198526, 2023. doi:10.3389/fcvm.2023.1198526

[15] N. Cahan et al., "Multimodal fusion models for pulmonary embolism mortality prediction," *Scientific Reports*, vol. 13, no. 1, p. 7544, 2023.
doi:10.1038/s41598-023-34303-8

[16] L. Z. Hou Yufen, "Diagnostic and Efficacy Criteria for Deep Venous Thrombosis of the Lower Extremities (Revised in 2015)," *Chin J Integr Tradit West Med Surgery* Zhong Guo Zhong Xi Yi Jie He Wai Ke Za Zhi, vol. 22, no. 5, pp. 520-520, 2016.

[17] F. Dentali et al., "Clinical course of isolated distal deep vein thrombosis in patients with active cancer: a multicenter cohort study," *Journal of thrombosis and haemostasis*, vol. 15, no. 9, pp. 1757-1763, 2017.
doi:10.1111/jth.13761

[18] P. C. Kruger, J. W. Eikelboom, J. D. Douketis, and G. J. Hankey, "Deep vein thrombosis: update on diagnosis and management," *Medical Journal of Australia*, vol. 210, no. 11, pp. 516-524, 2019.
doi:10.5694/mja2.50201

[19] F. Xing, L. Li, Y. Long, and Z. Xiang, "Admission prevalence of deep vein thrombosis in elderly Chinese patients with hip fracture and a new predictor based on risk factors for thrombosis screening," *BMC musculoskeletal disorders*, vol. 19, no. 1, p. 444, 2018. doi:10.1186/s12891-018-2371-5

[20] W. Li, Z. Chuanlin, M. Shaoyu, C. H. Yeh, C. Liqun, and Z. Zeju, "Catheter-directed thrombolysis for patients with acute lower extremity deep vein thrombosis: a meta-analysis," *Revista latino-americana de enfermagem*, vol. 26, p. e2990, 2018.
doi:10.1590/1518-8345.2309.2990

[21] S. Z. Goldhaber, E. A. Magnuson, K. M. Chinnakonddepalli, D. J. Cohen, and S. Vedantham, "Catheter-directed thrombolysis for deep vein thrombosis: 2021 update," *Vascular Medicine*, vol. 26, no. 6, pp. 662-669, 2021.
doi:10.1177/1358863X211042930

[22] X. Du et al., "Long-term outcome of catheter-directed thrombolysis in pregnancy-related venous thrombosis," *Medical Science Monitor: International Medical Journal of Experimental and Clinical Research*, vol. 25, p. 3771, 2019.
doi:10.12659/msm.914592

[23] M. J. Garcia et al., "Endovascular management of deep vein thrombosis with rheolytic thrombectomy: final report of the prospective multicenter PEARL (Peripheral Use of AngioJet Rheolytic Thrombectomy with a Variety of Catheter Lengths) registry," *Journal of Vascular and Interventional Radiology*, vol. 26, no. 6, pp. 777-785, 2015. doi:10.1016/j.jvir.2015.01.036

[24] H. İner, "The treatment indication affects the time in therapeutic range," *Cardiovascular Surgery and Interventions*, vol. 9, no. 3, pp. 147-151, 2022.
doi:10.5606/e-cvsi.2022.1392

[25] J. A. Kline, Z. P. Kahler, and D. M. Beam, "Outpatient treatment of low-risk venous thromboembolism with monotherapy oral anticoagulation: patient quality of life outcomes and clinician acceptance," *Patient preference and adherence*, pp. 561-569, 2016.
doi:10.2147/ppa.s104446

[26] A. Abdel-Hafez et al., "Predicting therapeutic response to unfractionated heparin therapy: machine learning approach," *Interactive Journal of Medical Research*, vol. 11, no. 2, p. e34533, 2022.
doi:10.2196/34533

[27] A. Shaikh et al., "Six-month outcomes of mechanical thrombectomy for treating deep vein thrombosis: analysis from the 500-patient CLOUT registry," *Cardiovascular and interventional radiology*, vol. 46, no. 11, pp. 1571-1580, 2023. doi:10.1007/s00270-023-03509-8

[28] M. Yao et al., "Neutrophil extracellular traps mediate deep vein thrombosis: from mechanism to therapy," *Frontiers in immunology*, vol. 14, p. 1198952, 2023.
doi:10.3389/fimmu.2023.1198952

[29] J. Ding, X. Yue, X. Tian, Z. Liao, R. Meng, and M. Zou, "Association between inflammatory biomarkers and venous thromboembolism: a systematic review and meta-analysis," *Thrombosis Journal*, vol. 21, no. 1, p. 82, 2023. doi:10.1186/s12959-023-00526-y

[30] N. Marlow, M. Eckert, G. Sharplin, I. Gwilt, and K. Carson-Chahhoud, "Graphical User Interface Development for a Hospital-Based Predictive Risk Tool: Protocol for a Co-Design Study," *JMIR Research Protocols*, vol. 12, no. 1, p. e47717, 2023.
doi:10.2196/47717

[31] S. Sachdeva et al., "Unraveling the role of cloud computing in health care system and biomedical sciences," *Heliyon*, vol. 10, no. 7, 2024.
doi:10.1016/j.heliyon.2024.e29044

[32] A. V. Ponce-Bobadilla, V. Schmitt, C. S. Maier, S. Mensing, and S. Stodtmann, "Practical guide to SHAP analysis: Explaining supervised machine learning model predictions in drug development," *Clinical and*

translational science, vol. 17, no. 11, p. e70056, 2024.
doi:10.1111/cts.70056

[33] I. D. Mienye et al., "A survey of explainable artificial intelligence in healthcare: Concepts, applications, and challenges," *Informatics in Medicine Unlocked*, vol. 51, p. 101587, 2024. doi:10.1016/j.imu.2024.101587

[34] J. S. Chang et al., "Continuous multimodal data supply chain and expandable clinical decision support for oncology," *npj Digital Medicine*, vol. 8, no. 1, p. 128, 2025. doi:10.1038/s41746-025-01508-2

[35] B. Vasey et al., "Reporting guideline for the early stage clinical evaluation of decision support systems driven by artificial intelligence: DECIDE-AI," *bmj*, vol. 377, 2022. doi:10.1038/s41591-022-01772-9



This article is an open-access article distributed under the terms and conditions of the Creative Commons Attribution (CC BY) license
(<https://creativecommons.org/licenses/by/4.0/>).